Research Square

Preprints are preliminary reports that have not undergone peer review.
They should not be considered conclusive, used to inform clinical practice,
or referenced by the media as validated information.

# Perfusion defect, but not CT-quantified emphysema burden, is associated with major adverse events in pulmonary emphysema: a short-time deep-inspiratory breath-hold SPECT/CT cohort study

**Teruhiko Hamana**
Nippon Medical School
**Yoshimitsu Fukushima**
fuku@nms.ac.jp
Nippon Medical School
**Kenji Yodogawa**
Nippon Medical School
**Takahiro Ando**
Nippon Medical School
**Yujiro Nakaoka**
Nippon Medical School
**Yoshimitsu Honda**
Nippon Medical School
**Satoshi Harashina**
Nippon Medical School Hospital
**Kyouji Asano**
Nippon Medical School Hospital
**Hiromitsu Hayashi**
Nippon Medical School
**Shinichiro Kumita**
Nippon Medical School

**Research Article**

**Keywords:** Pulmonary Emphysema, Tomography, Emission-Computed, Single-Photon, Perfusion Imaging, Pulmonary Circulation, Prognosis

**Posted Date:** August 28th, 2026

**DOI:** https://doi.org/10.21203/rs.3.rs-10489862/v1

**License:** This work is licensed under a Creative Commons Attribution 4.0 International License. Read Full License

**Additional Declarations:** No competing interests reported.

## Abstract

# Background

Computed tomography (CT) quantifies the structural burden of pulmonary emphysema, but outcomes are driven substantially by pulmonary vascular impairment, which structural indices do not measure. A short-time deep-inspiratory breath-hold (STDIBH) pulmonary perfusion single-photon emission computed tomography/computed tomography (SPECT/CT) technique developed by the authors enables accurate quantification of the percent perfusion defect (%PPD). This study evaluated whether %PPD is associated with major adverse events (MAE) in pulmonary emphysema, and whether the CT-quantified emphysema burden carried comparable prognostic information.

# Methods

Of 91 consecutive patients who underwent STDIBH pulmonary perfusion SPECT/CT, 74 were analyzed after exclusion of pulmonary thromboembolism, malignancy, or insufficient follow-up. The %PPD was perfusion defect volume on SPECT divided by anatomical lung volume on CT, and the percentage of low-attenuation area (%LAA) was measured on the same CT. The primary endpoint was MAE-free survival over the full follow-up. Kaplan-Meier analysis and Akaike information criterion-based Cox regression were used.

# Results

Patients (median age 70 years [IQR 64–76]; 57 male [77%]) were followed for a median of 70.9 months (reverse Kaplan-Meier). MAE occurred in 54 patients (73.0%). The optimal %PPD cutoff was 34.2% (AUC 0.776, 95% CI 0.64–0.90; sensitivity 81.5%; specificity 75.0%). High %PPD was associated with worse MAE-free survival (median 11.3 vs 80.6 months; log-rank $P < 0.001$), and %PPD remained independently associated with MAE on multivariable Cox regression (HR 1.0153 per 1%, equivalent to 1.1600 per 10% increase; 95% CI 1.0043–1.0264; $P = 0.006$) and in the heart-failure-inclusive sensitivity analysis (HR 1.0115, $P = 0.030$). The %LAA was not associated with MAE. In exploratory analysis, the %PPD − %LAA mismatch separated MAE-free survival (5-year landmark 15.0% vs 53.4%; log-rank $P = 0.002$).

# Conclusions

In pulmonary emphysema, functional perfusion impairment quantified by STDIBH pulmonary perfusion SPECT/CT was independently associated with major adverse events, whereas the CT-quantified structural emphysema burden was not. Risk tracked the functional rather than the structural component of the disease, and %PPD identified risk that structural CT alone left unresolved.

## Background

Pulmonary emphysema is characterized by irreversible alveolar wall destruction and distal airspace enlargement, leading to airflow limitation and impaired gas exchange [1]. It affects a substantial proportion of

patients with chronic obstructive pulmonary disease (COPD), and its global prevalence continues to rise [2]. CT-assessed emphysema severity predicts mortality independently of spirometric measures [3, 4], supporting imaging assessment beyond structural evaluation alone.

Pulmonary vascular impairment is increasingly recognized as a central feature of emphysema. Capillary destruction, hypoxic vasoconstriction, and endothelial dysfunction impair pulmonary perfusion and gas exchange [5, 6], and vascular dysfunction is associated with exercise intolerance, reduced quality of life, and mortality [7, 8]. It may be both a consequence of parenchymal destruction and an independent driver of progression [9, 10]. CT-derived vascular parameters provide indirect morphological surrogates [11], but direct functional assessment is needed to characterize the circulatory component of emphysema.

Pulmonary perfusion scintigraphy using $^{99m}$Tc-macroaggregated albumin ($^{99m}$Tc-MAA) is a well-established nuclear medicine technique for evaluating pulmonary blood flow distribution [12]. The integration of single-photon emission computed tomography/computed tomography (SPECT/CT) has enabled three-dimensional quantification of perfusion defects with anatomical correlation [13]. Conventional pulmonary perfusion SPECT/CT, however, is typically performed during tidal breathing, which may underestimate perfusion defects in emphysema due to incomplete lung inflation and respiratory motion artifacts.

Suga et al. pioneered the deep-inspiratory breath-hold (DIBrH) perfusion SPECT technique, demonstrating improved defect clarity in smokers' lungs [14] and with SPECT-CT fusion in pulmonary thromboembolism and emphysema [15, 16]. CT density-based attenuation correction further sharpens defect contrast [17]. Related ventilation approaches include respiratory-gated perfusion assessment [18], the $^{99m}$Tc-Technegas stripe sign [19], and automated V/Q quotient SPECT for V/Q imbalance in emphysema [20].

Perfusion SPECT/CT also has utility beyond diagnosis. Co-registered perfusion SPECT/CT predicts outcomes after lung volume reduction surgery [21], and ventilation/perfusion (V/P) SPECT detects early COPD changes, correlates with emphysema extent and spirometric function [22], and may identify COPD heterogeneity [23]. The percent perfusion defect (%PPD), calculated as perfusion defect volume divided by lung volume, provides a quantitative index of pulmonary circulatory function. A pilot study first applied it to assess pulmonary circulatory impairment in chronic lung disease (Atsumi et al. [24]).

The authors developed a novel short-time deep-inspiratory breath-hold (STDIBH) pulmonary perfusion SPECT/CT technique, not previously reported in the literature, that uses 12 repeated 10-second breath-hold acquisitions [25]. By suppressing respiratory motion and providing full-inspiration SPECT images with accurate SPECT-CT co-registration, the technique enables accurate quantification of %PPD, and it has shown prognostic value in pulmonary thromboembolism [25]. Its prognostic value in pulmonary emphysema has not been investigated.

We therefore evaluated whether %PPD derived from STDIBH pulmonary perfusion SPECT/CT is associated with major adverse events in pulmonary emphysema, and whether the CT-derived low-attenuation area, the established structural index, carries comparable prognostic information in the same patients. Exploratory analyses examined Meyer regional scores and perfusion–structure or ventilation–perfusion mismatch metrics.

# Methods

# Study design and patient selection

This single-center, retrospective observational study was conducted at Nippon Medical School Hospital. Consecutive patients with CT-diagnosed pulmonary emphysema who underwent STDIBH pulmonary perfusion SPECT/CT between May 2012 and March 2023 were screened. Exclusion criteria were known pulmonary embolism, prior lung resection surgery, active pulmonary malignancy affecting perfusion assessment, inability to perform breath-hold maneuvers, and death from malignancy or pulmonary thromboembolism during follow-up.

This study was performed in accordance with the principles of the Declaration of Helsinki. The study protocol was approved by the Central Ethics Committee of Nippon Medical School (Reference No. M-2026-544). The requirement for written informed consent was waived due to the retrospective nature of the study, and an opt-out method was employed for patient enrollment.

## STDIBH pulmonary perfusion SPECT/CT

Pulmonary perfusion SPECT/CT was performed using a dual-head SPECT/CT system (Symbia T2; Siemens Healthineers) with low-energy high-resolution collimators. $^{99m}$Tc-MAA was administered in two divided doses (185 MBq supine and 185 MBq prone; total 370 MBq). SPECT acquisition began 10 minutes after the second dose. The STDIBH protocol used 12 repeated 10-second deep-inspiratory breath-hold acquisitions during 360° continuous detector rotation with a 128 × 128 matrix and approximately 10-second recovery intervals. At least 8 adequate acquisitions were required for composite reconstruction.

Low-dose CT was performed for attenuation correction and anatomical correlation during a single deep-inspiratory breath-hold matched to the SPECT acquisition (tube voltage 110 kV, tube current 10–40 mAs, slice thickness 5 mm). SPECT images were reconstructed using the Flash-3D iterative algorithm (Siemens Healthineers) with 8 iterations and 6 subsets, incorporating CT-based attenuation correction, triple-energy-window scatter correction, and resolution recovery. Reconstructed SPECT and co-registered CT images were fused using the syngo Fusion Package (Siemens Healthineers) for clinical interpretation.

## Image analysis

# #### Percent perfusion defect (%PPD)

Quantitative analysis was performed on the syngo workstation (Siemens Healthineers) using the semi-automated, threshold-based volumetric perfusion-defect quantification previously described for STDIBH pulmonary perfusion SPECT/CT [25]. The %PPD was calculated as follows:

> %PPD = (perfusion defect volume on SPECT / anatomical lung volume on CT) × 100

Perfusion defect volume was defined as SPECT voxels with tracer uptake below 31% of the maximum pulmonary uptake, a threshold calibrated so that the mean %PPD in normal controls was 0% [25]. Anatomical lung volume was segmented from co-registered CT using attenuation between − 1024 and − 400 Hounsfield

units, retaining emphysematous low-attenuation parenchyma in the %PPD denominator. %PPD was calculated for the total lung and each lung separately.

### #### Meyer regional defect scores (Meyer P-score and Meyer V-score)

For region-based assessment, planar pulmonary perfusion images were divided into six anatomical zones by visually trisecting each lung. Relative uptake in each zone was scored as 1.0 (normal relative to the most-preserved zone in the same patient), 0.75, 0.50, 0.25, or 0 (absent). The Meyer P-score (%) was calculated as the volume-weighted total deficiency:

> **Meyer P-score = $(1 - \Sigma_i\, w_i \times u_i) \times 100$**

where $u_i$ is the relative uptake in zone i and $w_i$ is the regional volume weight (right upper 0.18, right middle 0.12, right lower 0.25, left upper 0.13, left middle 0.12, left lower 0.20; $\Sigma\, w_i = 1.00$). Higher values indicate greater perfusion impairment. The same framework was applied to planar $^{81m}$Kr gas ventilation scintigraphy to compute the Meyer V-score in 46 patients with paired ventilation imaging. A single board-certified nuclear medicine physician, blinded to clinical and outcome data, performed all scoring.

### #### Percent low-attenuation area (%LAA)

The percentage of low-attenuation area (%LAA) was quantified from the same low-dose CT acquisition used for attenuation correction. %LAA was defined as the fraction of total lung voxels below − 950 Hounsfield units and expressed as a percentage of total lung volume.

### #### Perfusion–structure and ventilation–perfusion mismatch metrics

Two post hoc mismatch metrics were calculated: perfusion–structure mismatch (%PPD − %LAA) in all 74 patients and ventilation–perfusion mismatch (Meyer P-score − Meyer V-score) in the 46 patients with paired ventilation imaging, with positive values indicating perfusion impairment exceeding the structural or ventilation reference. These exploratory metrics were evaluated descriptively and in univariable analyses, with the multivariable %PPD-anchored Cox model as the prespecified analytic primary.

## Clinical outcomes

The primary endpoint was MAE-free survival. MAE was defined as all-cause death, hospitalization for respiratory failure, AECOPD hospitalization, or new home oxygen therapy (HOT). HF hospitalization was excluded from the primary composite because it was driven by cardiac comorbidities rather than emphysema severity, and %PPD did not predict HF hospitalization (univariable HR 0.9946, $P = 0.576$). A 5-component composite including HF hospitalization was evaluated as a prespecified sensitivity analysis. Follow-up was open-ended, extending to the last clinical contact without administrative censoring.

## Statistical analysis

Continuous variables were expressed as mean ± standard deviation (SD) for normally distributed data and median (interquartile range [IQR]) for non-normally distributed data. Categorical variables were expressed as frequencies and percentages. Normality was assessed using the Shapiro-Wilk test. Comparisons between groups were performed using the unpaired t-test or Mann-Whitney U test for continuous variables and the chi-square test or Fisher's exact test for categorical variables, as appropriate.

Median follow-up was estimated by the reverse Kaplan-Meier method. The optimal %PPD cutoff for MAE was determined by ROC analysis using the Youden index, with the area under the curve (AUC) and a bootstrap 95% confidence interval (CI). MAE-free survival was estimated by Kaplan-Meier analysis and compared by the log-rank test. Univariable Cox regression was performed for prespecified predictors, with descriptive *P* values and no multiplicity correction. Multivariable models were selected by AIC-based best-subset search among variables with univariable $P < 0.20$, within the complete-case events-per-variable limit. The most parsimonious model with all covariates significant on the full cohort was retained as the primary model. Hazard ratios (HR) are reported with 95% CIs and, for %PPD, per 10% and per interquartile range. The proportional-hazards assumption was checked with scaled Schoenfeld residuals, model optimism by a 1,000-replication bootstrap (optimism-corrected concordance index), and robustness to repeated examinations in 7 patients by cluster-robust (patient-level) standard errors.

Mismatch metrics were evaluated as univariable Cox predictors and in bivariable models with %PPD and the corresponding structural or ventilation reference, compared by AIC and Harrell's concordance index. Median-split Kaplan-Meier analyses were descriptive. Because the mismatch metrics, %PPD cutoff, and bivariable models were derived and evaluated in the same dataset, all effect sizes require external validation.

A two-tailed $P < 0.05$ was considered statistically significant. Statistical analyses were performed using Python 3 with the lifelines (version 0.30) and scikit-learn (version 1.8) packages.

Claude Code (Anthropic), a large language model tool, was used for manuscript formatting, reference list preparation, and drafting assistance. It was not used to generate, analyze, or interpret data. The authors reviewed and edited all such content and take full responsibility for the publication.

## Results

# Patient characteristics

Of 91 patients initially identified, 17 were excluded (pulmonary thromboembolism, n = 9; malignancy, n = 7; insufficient follow-up data, n = 1), yielding 74 patients for analysis (Fig. 1, Table 1). Median age was 70 years (IQR 64–76), and 57 patients (77.0%) were male. Interstitial pneumonia was present in 26 patients (35.1%), and pulmonary hypertension (TRPG > 31 mmHg) [26] in 39 of 68 patients with measurable TRPG (57.4%).

Table 1
Baseline characteristics of the study population (n = 74)

| Variable | Total (n = 74) |
|---|---|
| **Demographics** | |
| Age (years) | 69.5 ± 10.3 |
| Male sex, n (%) | 57 (77.0%) |
| BMI (kg/m²) | 22.3 ± 4.9 |
| **Smoking history** | |
| Smoking status (current / ex / never) | current 1 (1.4%) / ex 61 (82.4%) / never 12 (16.2%) |
| Pack-years | 43.0 [24.7–64.0] |
| **Pulmonary function** | |
| %VC (%) (n = 73) | 81.4 [67.7–96.2] |
| %FEV1.0 (%) (n = 73) | 85.0 [59.1–106.5] |
| FEV1.0/FVC (%) (n = 73) | 73.6 [56.4–84.0] |
| %DLCO (%) (n = 55) | 40.1 [26.6–61.8] |
| GOLD stage (1 / 2 / 3 / 4), n (%) | 41 (55.4%) / 20 (27.0%) / 9 (12.2%) / 4 (5.4%) |
| **Cardiac function** | |
| LVEF (%) (n = 71) | 71.0 [62.5–75.0] |
| RVEF (%) (n = 73) | 39.0 [31.9–50.0] |
| TRPG (mmHg) (n = 68) | 36.6 [23.9–52.0] |
| Heart rate (bpm) | 70.0 [63.0–79.0] |
| **Laboratory data** | |
| BNP (pg/mL) | 229.8 [59.8–609.8] |
| $SaO_2$ (%) | 91.5 [85.7–95.5] |
| Creatinine (mg/dL) | 0.8 [0.6–1.2] |
| eGFR (mL/min/1.73 m²) | 70.0 [42.7–88.6] |
| **Comorbidities, n (%)** | |
| Coronary artery disease | 8 (10.8%) |

*Data are mean ± SD, median [IQR], or n (%). ACE, angiotensin-converting enzyme; BNP, B-type natriuretic peptide; CKD, chronic kidney disease; DLCO, diffusing capacity for carbon monoxide; eGFR, estimated glomerular filtration rate; FEV1.0/FVC, forced expiratory volume in 1 second / forced vital capacity; HOT, home oxygen therapy; LVEF, left ventricular ejection fraction; RVEF, right ventricular ejection fraction; TRPG, tricuspid regurgitation pressure gradient.*

| Variable | Total (n = 74) |
|---|---|
| **Demographics** | |
| Hypertension | 33 (44.6%) |
| Dyslipidemia | 20 (27.0%) |
| Diabetes mellitus | 17 (23.0%) |
| CKD (eGFR < 60) | 29 (39.2%) |
| Pulmonary hypertension (TRPG > 31 mmHg) (n = 68) | 39 (57.4%) |
| Atrial fibrillation | 12 (16.2%) |
| Interstitial pneumonia | 26 (35.1%) |
| HOT use at baseline | 34 (45.9%) |
| **Medications, n (%)** | |
| Calcium-channel blocker | 26 (35.1%) |
| Angiotensin-receptor blocker | 16 (21.6%) |
| ACE inhibitor | 8 (10.8%) |
| Spironolactone | 10 (13.5%) |
| Beta-blocker | 12 (16.2%) |
| Statin | 18 (24.3%) |

*Data are mean ± SD, median [IQR], or n (%). ACE, angiotensin-converting enzyme; BNP, B-type natriuretic peptide; CKD, chronic kidney disease; DLCO, diffusing capacity for carbon monoxide; eGFR, estimated glomerular filtration rate; FEV1.0/FVC, forced expiratory volume in 1 second / forced vital capacity; HOT, home oxygen therapy; LVEF, left ventricular ejection fraction; RVEF, right ventricular ejection fraction; TRPG, tricuspid regurgitation pressure gradient.*

# %PPD and group comparison

The median %PPD was 44.8% (IQR 31.7–68.9; Table 2). Based on ROC analysis, the optimal cutoff value for %PPD to predict MAE was 34.2% (AUC 0.776, 95% CI 0.64–0.90; sensitivity 81.5%; specificity 75.0%; Youden index 0.565) (Fig. 2). Patients were classified into the low %PPD group (n = 25, %PPD < 34.2%) and the high %PPD group (n = 49, %PPD ≥ 34.2%).

Table 2
STDIBH pulmonary perfusion SPECT/CT imaging parameters and outcomes (n = 74)

| Variable | Total (n = 74) |
|---|---|
| **Imaging: SPECT/CT perfusion** | |
| %PPD, total (%) | 44.8 [31.7–68.9] |
| Meyer P-score (%) | 41.4 [28.1–61.1] |
| Meyer V-score (%) (n = 46) | 17.1 [8.8–28.5] |
| **Imaging: CT quantitative** | |
| %LAA (%) | 5.9 [1.6–12.8] |
| **Imaging: perfusion–structure mismatch** | |
| %PPD − %LAA (%) | 36.9 [26.0–48.4] |
| Meyer P − V mismatch (%) (n = 46) | 26.6 [7.7–36.7] |
| **Follow-up** | |
| Follow-up, months (reverse Kaplan-Meier) | 70.9 [45.9–125.1] |
| SPECT/CT date range | May 2012 – March 2023 |
| **Events (primary 4-component MAE), n (%)** | |
| MAE (composite) | 54 (73.0%) |
| All-cause death | 37 (50.0%) |
| RF hospitalization | 37 (50.0%) |
| AECOPD hospitalization | 28 (37.8%) |
| HOT introduction | 10 (13.5%) |
| HF hospitalization (sensitivity) | 19 (25.7%) |

*Data are median [IQR] or n (%). MAE = all-cause death + RF hospitalization + AECOPD hospitalization + HOT introduction. AECOPD, acute exacerbation of chronic obstructive pulmonary disease; HF, heart failure; HOT, home oxygen therapy; %LAA, percentage of low-attenuation area; %PPD, percent perfusion defect; RF, respiratory failure; STDIBH, short-time deep-inspiratory breath-hold.*

Baseline characteristics are summarized in Table 1. Confounder adjustment was handled through the prespecified multivariable Cox framework rather than dichotomized group comparisons, which would inherit optimism from the data-derived cutoff.

# Major adverse events

Over a median follow-up of 70.9 months (reverse Kaplan-Meier; IQR 45.9–125.1), MAE occurred in 54 patients (73.0%). Follow-up reached a primary event or the 5-year landmark in 63 patients (85%). Component events were all-cause death in 37 patients (50.0%), respiratory-failure hospitalization in 37 (50.0%), AECOPD

hospitalization in 28 (37.8%), and new HOT introduction in 10 patients (13.5%). MAE incidence was higher in the high %PPD group than in the low %PPD group (89.8% vs 40.0%; $P < 0.001$).

# Survival analysis

Kaplan-Meier analysis demonstrated markedly worse MAE-free survival in the high %PPD group than in the low %PPD group (median 11.3 vs 80.6 months; 5-year landmark 17.3% vs 69.6%; log-rank $P < 0.001$) (Fig. 3).

On univariable Cox regression, %PPD was associated with MAE (HR 1.0147 per 1% increase, $P = 0.007$). Significant nonimaging predictors are listed in Table 3. Meyer P-score and Meyer V-score were also associated with MAE, whereas %LAA was not.

Table 3
Selected Cox regression results for the prediction of MAE

| Variable | HR | 95% CI | P value | HR | 95% CI | P value |
|---|---|---|---|---|---|---|
| | Univariable | Univariable | Univariable | Multivariable | Multivariable | Multivariable |
| **Final multivariable covariates** | | | | | | |
| %PPD, total (per 1% increase) | 1.0147 | 1.0040–1.0254 | 0.0068 | 1.0153 | 1.0043–1.0264 | 0.0063 |
| BNP (per 100 pg/mL) | 1.0218 | 1.0099–1.0339 | 0.0003 | 1.0219 | 1.0099–1.0340 | 0.0003 |
| Interstitial pneumonia | 2.3739 | 1.3272–4.2461 | 0.0036 | 2.4153 | 1.3418–4.3475 | 0.0033 |
| **Selected univariable predictors** | | | | | | |
| TRPG (per mmHg) | 1.0275 | 1.0121–1.0431 | 0.0004 | | | |
| Pulmonary hypertension | 1.9159 | 1.0793–3.4013 | 0.0264 | | | |
| Atrial fibrillation | 0.3639 | 0.1551–0.8539 | 0.0202 | | | |
| %DLCO (per %) | 0.9786 | 0.9633–0.9943 | 0.0075 | | | |
| RVEF (per %) | 0.9769 | 0.9550–0.9993 | 0.0438 | | | |
| HOT use at baseline | 2.0676 | 1.1936–3.5816 | 0.0096 | | | |
| FEV1.0/FVC (per %) | 1.0073 | 0.9938–1.0209 | 0.2911 | | | |
| **Exploratory imaging metrics** | | | | | | |
| Meyer P-score (per 1% increase) | 1.0188 | 1.0062–1.0315 | 0.0033 | | | |

*Multivariable model: AIC = 364.9, concordance index = 0.702 (bootstrap optimism-corrected 0.69); the proportional-hazards assumption was satisfied (Schoenfeld P ≥ 0.47). For interpretability, the multivariable %PPD HR corresponds to 1.16 per 10% and 1.76 per interquartile range. Rows show final model covariates, clinically interpreted predictors, and exploratory imaging metrics. HR, hazard ratio; CI, confidence interval; BNP, B-type natriuretic peptide; FEV1.0/FVC, forced expiratory volume in 1 second / forced vital capacity; %LAA, percentage of low-attenuation area; %PPD, percent perfusion defect; TRPG, tricuspid regurgitation pressure gradient.*

| Variable | HR | 95% CI | P value | HR | 95% CI | P value |
|---|---|---|---|---|---|---|
| | Univariable | Univariable | Univariable | Multivariable | Multivariable | Multivariable |
| **Final multivariable covariates** | | | | | | |
| Meyer V-score (per 1% increase) (n = 46) | 1.0257 | 1.0030–1.0490 | 0.0263 | | | |
| %LAA (per 1% increase) | 1.0080 | 0.9884–1.0280 | 0.4246 | | | |
| %PPD – %LAA (per 1% increase) | 1.0215 | 1.0077–1.0355 | 0.0022 | | | |
| Meyer P – V mismatch (per 1% increase) (n = 46) | 1.0283 | 1.0078–1.0493 | 0.0067 | | | |
| *Multivariable model: AIC = 364.9, concordance index = 0.702 (bootstrap optimism-corrected 0.69); the proportional-hazards assumption was satisfied (Schoenfeld P ≥ 0.47). For interpretability, the multivariable %PPD HR corresponds to 1.16 per 10% and 1.76 per interquartile range. Rows show final model covariates, clinically interpreted predictors, and exploratory imaging metrics. HR, hazard ratio; CI, confidence interval; BNP, B-type natriuretic peptide; FEV1.0/FVC, forced expiratory volume in 1 second / forced vital capacity; %LAA, percentage of low-attenuation area; %PPD, percent perfusion defect; TRPG, tricuspid regurgitation pressure gradient.* | | | | | | |

In exploratory perfusion–structure analysis, %LAA acquired a paradoxically protective effect when entered with %PPD, while %PPD remained a strong predictor. The equivalent %PPD – %LAA mismatch was a stronger univariable predictor than %PPD alone (AIC 376.9 vs 378.8; concordance 0.670 vs 0.643). Patients with a mismatch above the median had worse MAE-free survival (5-year landmark 15.0% vs 53.4%, log-rank *P* = 0.002).

The primary multivariable model (%PPD, BNP, and interstitial pneumonia) was fit on the full cohort (n = 74, EPV 18); TRPG, significant univariably, was non-significant and collinear with pulmonary hypertension (r = 0.86) and was not retained. %PPD remained an independent predictor of MAE (HR 1.0153 per 1% increase, equivalent to 1.1600 per 10%, 95% CI 1.0043–1.0264, *P* = 0.006), along with BNP and interstitial pneumonia (Table 3). The proportional-hazards assumption held for all covariates, and %PPD remained significant after bootstrap optimism correction (corrected concordance index 0.690) and with cluster-robust standard errors (HR 1.0153, *P* = 0.003).

# Sensitivity analysis

In a prespecified 5-component MAE sensitivity analysis including HF hospitalization, 56 events (75.7%) occurred. Only 2 of the 19 patients with HF hospitalization had no other qualifying component. The association between %PPD and MAE was attenuated but remained significant (univariable HR 1.0115, 95% CI 1.0011–

1.0220, *P* = 0.030; AUC 0.759), reflecting HF events associated with cardiac comorbidities rather than emphysema severity.

## Discussion

STDIBH pulmonary perfusion SPECT/CT quantified pulmonary circulatory impairment in emphysema, and %PPD was independently associated with major adverse events after adjustment for BNP and interstitial pneumonia. The CT-derived emphysema burden, measured in the same patients, carried no such signal.

# Pulmonary vascular impairment in emphysema

Perfusion impairment in emphysema is multifactorial. Capillary destruction accompanies alveolar wall loss, and hypoxic vasoconstriction and endothelial dysfunction further compromise perfusion [5]. Pulmonary vascular disease in COPD may reflect endothelial injury and vascular remodeling rather than a passive consequence of parenchymal destruction [9, 10, 27]. Smoke-induced endothelial apoptosis contributes independently of airway disease [28], and restoring pulmonary endothelial cells can reverse emphysematous changes [29].

# Quantitative perfusion assessment by STDIBH SPECT/CT

STDIBH maximizes lung inflation, suppresses respiratory motion artifacts, and improves SPECT–CT co-registration, enabling accurate volumetric quantification of %PPD [14–17]. Repeated 10-second breath-holds minimize discomfort and preserve count statistics, supporting %PPD as an integrated measure of capillary destruction and functional vasoconstriction.

# Functional perfusion versus structural emphysema burden

Whether CT-defined structural burden or SPECT-defined functional perfusion better captures risk is a key question in emphysema prognostication. In this cohort, %PPD was associated with MAE on univariable and multivariable analysis, and Meyer P-score was also predictive (Table 3), whereas %LAA showed no detectable prognostic signal. This dissociation suggests the prognostic value of perfusion impairment is not reducible to CT-visible airspace destruction [9, 27, 28].

Joint modeling supported this dissociation. With %PPD and %LAA entered together, %PPD remained predictive, whereas %LAA acquired a paradoxically protective effect (Table 3), and the equivalent %PPD − %LAA mismatch had lower AIC and higher concordance than %PPD alone, suggesting that risk concentrates in perfusion impairment not explained by CT-visible emphysema (Fig. 4). This interpretation remains exploratory because the bivariable model and mismatch reparameterization are mathematically related.

# Ventilation–perfusion mismatch as a prognostic refinement

In the 46 patients with paired ventilation imaging, the Meyer P − V mismatch (median 26.6%, IQR 7.7–36.7%) was associated with MAE univariably but lost significance after %PPD adjustment, indicating no incremental stratification.

# Prognostic value of %PPD

The %PPD–MAE association is consistent with evidence linking pulmonary vascular dysfunction to adverse outcomes in COPD. CT-derived surrogates such as pulmonary arterial enlargement [7] and small pulmonary vessel area [11] predict exacerbations and disease severity but remain indirect morphological signals, whereas %PPD from STDIBH SPECT/CT adds direct functional assessment. A pilot study established %PPD as a marker of pulmonary hypertension in chronic lung disease (Atsumi et al. [24]), and the present study extends this to prognosis in emphysema.

The difference in MAE incidence suggests that %PPD identifies a high-risk emphysema phenotype with disproportionate pulmonary circulatory impairment. Although cardiovascular comorbidity contributes to COPD morbidity [30] and pulmonary hypertension classification distinguishes cardiac from pulmonary etiologies [31], the data support a respiratory-focused composite because HF events, driven by cardiac comorbidities, may dilute the pulmonary-specific signal.

# Clinical implications

High %PPD may identify patients needing closer monitoring, pulmonary rehabilitation, pulmonary hypertension screening, or targeted intervention. Because exacerbation frequency predicts subsequent events [32], combining %PPD with clinical risk factors may improve prognostic stratification.

# Limitations

Limitations include the retrospective single-center design, no prospective power calculation, internal derivation of the 34.2% cutoff, descriptive univariable Cox tests without multiplicity correction, incomplete pulmonary function data, %LAA measurement from 5-mm low-dose attenuation-correction CT rather than thin-section CT, residual timing misclassification, no competing-risk analysis, single-reader quantification, repeated examinations in 7 patients, and no non-breath-hold comparator. Cluster-robust analysis showed no material effect on %PPD.

## Conclusions

In pulmonary emphysema, this STDIBH pulmonary perfusion SPECT/CT technique quantified functional perfusion impairment, and %PPD was independently associated with respiratory-focused major adverse events and with worse MAE-free survival, whereas the CT-derived structural emphysema burden showed no association with outcome. Risk tracked the functional rather than the structural component of the disease. Perfusion, rather than structure, marked the patients whom CT-quantified emphysema burden left unstratified.

## Abbreviations

AECOPD
acute exacerbation of chronic obstructive pulmonary disease
AIC
Akaike information criterion
AUC
area under the curve
BNP

B-type natriuretic peptide
CI
confidence interval
COPD
chronic obstructive pulmonary disease
DIBrH
deep-inspiratory breath-hold
EPV
events per variable
HF
heart failure
HOT
home oxygen therapy
HR
hazard ratio
IQR
interquartile range
%LAA
percentage of low-attenuation area
MAA
macroaggregated albumin
MAE
major adverse event
%PPD
percent perfusion defect
ROC
receiver operating characteristic
SD
standard deviation
SPECT/CT
single-photon emission computed tomography/computed tomography
STDIBH
short-time deep-inspiratory breath-hold
TRPG
tricuspid regurgitation pressure gradient
V/P
ventilation/perfusion (imaging)
V/Q
ventilation/perfusion (ratio).

# Declarations

### Ethics approval and consent to participate

This study was performed in accordance with the principles of the Declaration of Helsinki. The study protocol was approved by the Central Ethics Committee of Nippon Medical School (Reference No. M-2026-544). The requirement for written informed consent was waived due to the retrospective nature of the study, and an opt-out method was employed for patient enrollment.

**Consent for publication**

Not applicable. All imaging data are de-identified, and no individually identifiable patient information is presented.

# Competing interests

The authors declare that they have no competing interests.

# Funding

# Author Contribution

Contributions follow the CRediT taxonomy. TH and YF contributed equally and share first authorship. TH: Conceptualization; Methodology; Formal analysis; Investigation; Data curation; Visualization; Writing – original draft; Writing – review & editing. YF: Conceptualization; Methodology; Formal analysis; Investigation; Data curation; Visualization; Supervision; Writing – original draft; Writing – review & editing. KY: Investigation; Validation; Writing – review & editing. TA: Investigation; Validation; Writing – review & editing. YN: Investigation; Data curation; Writing – review & editing. YH: Investigation; Data curation; Writing – review & editing. SH: Investigation; Resources; Writing – review & editing. KA: Investigation; Resources; Writing – review & editing. HH: Investigation; Methodology; Writing – review & editing. SK: Resources; Supervision; Writing – review & editing. All authors read and approved the final manuscript and agree to be accountable for all aspects of the work.

# Acknowledgement

The authors thank the physicians of the Department of Pulmonology for the clinical care and follow-up of the study patients, and the SPECT/CT technologists of the Department of Radiology for their assistance with short-time deep-inspiratory breath-hold image acquisition.

# Availability of data and materials

## References

1. Agustí A, Celli BR, Criner GJ, Halpin D, Anzueto A, Barnes P, et al. Global Initiative for Chronic Obstructive Lung Disease 2023 Report: GOLD Executive Summary. Am J Respir Crit Care Med. 2023;207:819–37.

2. Adeloye D, Chua S, Lee C, Basquill C, Papana A, Theodoratou E, et al. Global and regional estimates of COPD prevalence: Systematic review and meta-analysis. J Glob Health. 2015;5:020415.
3. Haruna A, Muro S, Nakano Y, Ohara T, Hoshino Y, Ogawa E, et al. CT scan findings of emphysema predict mortality in COPD. Chest. 2010;138:635–40.
4. Johannessen A, Skorge TD, Bottai M, Grydeland TB, Nilsen RM, Coxson H, et al. Mortality by level of emphysema and airway wall thickness. Am J Respir Crit Care Med. 2013;187:602–8.
5. Barberà JA, Peinado VI, Santos S. Pulmonary hypertension in chronic obstructive pulmonary disease. Eur Respir J. 2003;21:892–905.
6. Voelkel NF, Gomez-Arroyo J, Mizuno S. COPD/emphysema: The vascular story. Pulm Circ. 2011;1:320–6.
7. Wells JM, Washko GR, Han MK, Abbas N, Nath H, Mamary AJ, et al. Pulmonary arterial enlargement and acute exacerbations of COPD. N Engl J Med. 2012;367:913–21.
8. Estépar RS, Kinney GL, Black-Shinn JL, Bowler RP, Kindlmann GL, Ross JC, et al. Computed tomographic measures of pulmonary vascular morphology in smokers and their clinical implications. Am J Respir Crit Care Med. 2013;188:231–9.
9. Blanco I, Torres-Castro R, Barberà JA. Pulmonary vascular disease in chronic lung diseases: cause or comorbidity? Curr Opin Pulm Med. 2024;30:437–43.
10. Barr RG. The epidemiology of vascular dysfunction relating to chronic obstructive pulmonary disease and emphysema. Proc Am Thorac Soc. 2011;8:522–7.
11. Matsuoka S, Washko GR, Dransfield MT, Yamashiro T, San Jose Estepar R, Diaz A, et al. Quantitative CT measurement of cross-sectional area of small pulmonary vessel in COPD: correlations with emphysema and airflow limitation. Acad Radiol. 2010;17:93–9.
12. Bajc M, Schümichen C, Grüning T, Lindqvist A, Le Roux PY, Alatri A, et al. EANM guideline for ventilation/perfusion single-photon emission computed tomography (SPECT) for diagnosis of pulmonary embolism and beyond. Eur J Nucl Med Mol Imaging. 2019;46:2429–51.
13. Roach PJ, Schembri GP, Bailey DL. V/Q scanning using SPECT and SPECT/CT. J Nucl Med. 2013;54:1588–96.
14. Suga K, Yasuhiko K, Iwanaga H, Hayashi N, Yamashita T, Matsunaga N. Enhanced perfusion defect clarity and inhomogeneity in smokers' lungs with deep-inspiratory breath-hold perfusion SPECT images. Nucl Med Commun. 2005;26:801–7.
15. Suga K, Kawakami Y, Iwanaga H, Tokuda O, Matsunaga N. Automated breath-hold perfusion SPECT/CT fusion images of the lungs. AJR Am J Roentgenol. 2007;189:455–63.
16. Suga K, Kawakami Y, Iwanaga H, Hayashi N, Seto A, Matsunaga N. Assessment of anatomic relation between pulmonary perfusion and morphology in pulmonary emphysema with breath-hold SPECT-CT fusion images. Ann Nucl Med. 2008;22:339–47.
17. Suga K, Okada M, Kunihiro M, Iwanaga H, Matsunaga N. Clinical significance of CT density-based, non-uniform photon attenuation correction of deep-inspiratory breath-hold perfusion SPECT. Ann Nucl Med. 2011;25:289–98.
18. Kawakami Y, Suga K, Zaki M, Iwanaga H, Yamashita T, Hayashi N, et al. Semi-quantitation of pulmonary perfusion heterogeneity on respiratory-gated inspiratory and expiratory perfusion SPECT in patients with pulmonary emphysema. Ann Nucl Med. 2007;21:577–84.

19. Suga K, Kawakami Y, Iwanaga H, Tokuda O, Matsunaga N. A stripe sign on 99mTc-Technegas SPECT in pulmonary emphysema. Nucl Med Commun. 2008;29:553–61.
20. Suga K, Kawakami Y, Koike H, Iwanaga H, Tokuda O, Okada M, et al. Lung ventilation-perfusion imbalance in pulmonary emphysema: assessment with automated V/Q quotient SPECT. Ann Nucl Med. 2010;24:269–77.
21. Takenaka D, Ohno Y, Koyama H, Nogami M, Onishi Y, Matsumoto K, et al. Co-registered perfusion SPECT/CT: utility for prediction of improved postoperative outcome in lung volume reduction surgery candidates. Eur J Radiol. 2010;74:465–72.
22. Jögi J, Ekberg M, Jonson B, Bozovic G, Bajc M. Ventilation/perfusion SPECT in chronic obstructive pulmonary disease: an evaluation by reference to symptoms, spirometric lung function and emphysema, as assessed with HRCT. Eur J Nucl Med Mol Imaging. 2011;38:1344–52.
23. Bajc M, Chen Y, Wang J, Li XY, Shen WM, Wang CZ, et al. Identifying the heterogeneity of COPD by V/P SPECT: a new tool for improving the diagnosis of parenchymal defects and grading the severity of small airways disease. Int J Chron Obstruct Pulmon Dis. 2017;12:1579–87.
24. Atsumi K, Fukushima Y, Tanaka Y, Nishima S, Tanaka T, Seike M, et al. Novel evaluation of pulmonary hypertension associated with chronic lung disease using perfusion SPECT/CT: A pilot study. Pulm Circ. 2024;14:e12423.
25. Fukushima Y, Yodogawa K, Ando T, Honda Y, Hayashi H, Kumita S. Prognostic Value of Short-Time Deep-Inspiratory Breath-Hold Pulmonary Perfusion SPECT/CT for Patients with Pulmonary Thromboembolism. Ann Nucl Cardiol. 2026. 10.17996/anc.25-00013.
26. Humbert M, Kovacs G, Hoeper MM, Badagliacca R, Berger RMF, Brida M, et al. 2022 ESC/ERS Guidelines for the diagnosis and treatment of pulmonary hypertension. Eur Heart J. 2022;43:3618–731.
27. Polverino F, Celli BR, Owen CA. COPD as an endothelial disorder: endothelial injury linking lesions in the lungs and other organs? (2017 Grover Conference Series). Pulm Circ. 2018;8:2045894018758528.
28. Weissmann N. Chronic Obstructive Pulmonary Disease and Pulmonary Vascular Disease. A Comorbidity? Ann Am Thorac Soc. 2018;15(Suppl 4):S278–81.
29. Hisata S, Racanelli AC, Kermani P, Schreiner R, Houghton S, Palikuqi B, et al. Reversal of emphysema by restoration of pulmonary endothelial cells. J Exp Med. 2021;218:e20200938.
30. Alter P, Lucke T, Watz H, Andreas S, Kahnert K, Trudzinski FC, et al. Cardiovascular predictors of mortality and exacerbations in patients with COPD. Sci Rep. 2022;12:21882.
31. Simonneau G, Robbins IM, Beghetti M, Channick RN, Delcroix M, Denton CP, et al. Updated clinical classification of pulmonary hypertension. J Am Coll Cardiol. 2009;54(1 Suppl):S43–54.
32. Hurst JR, Vestbo J, Anzueto A, Locantore N, Müllerova H, Tal-Singer R, et al. Susceptibility to exacerbation in chronic obstructive pulmonary disease. N Engl J Med. 2010;363:1128–38.

## Figures

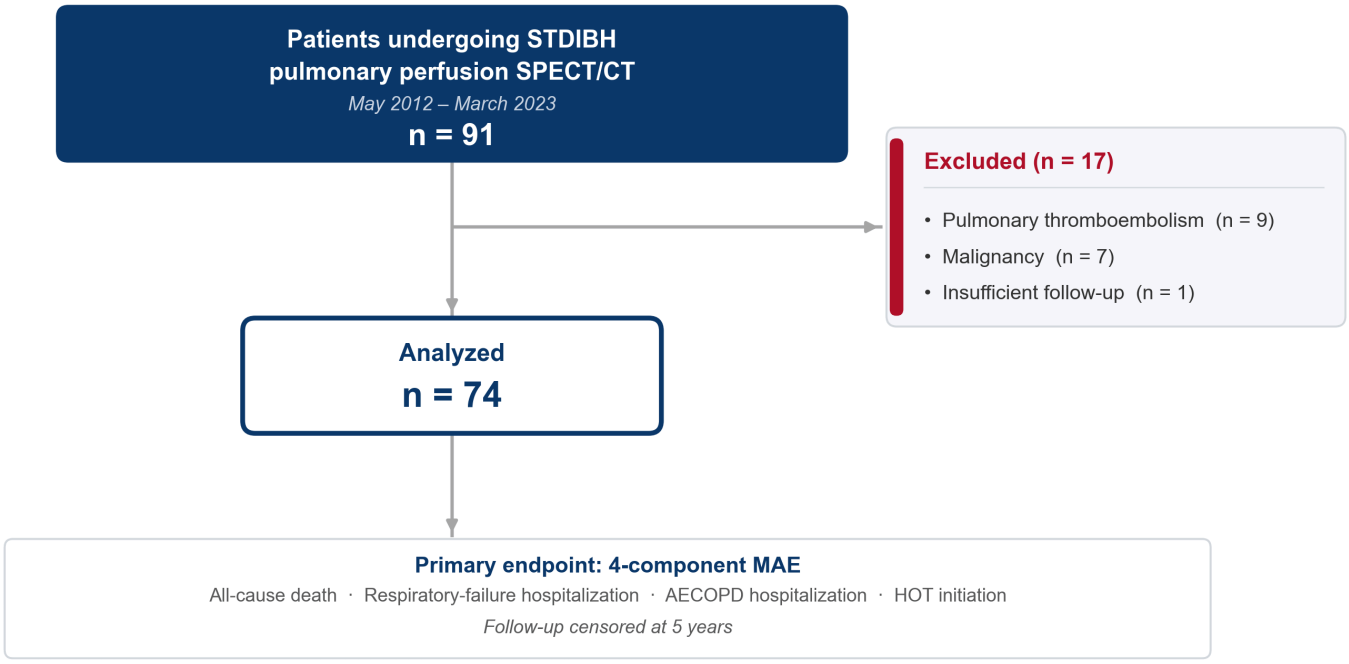



**Figure 1**

Patient flow diagram. Of 91 patients who underwent STDIBH pulmonary perfusion SPECT/CT, 17 were excluded (pulmonary thromboembolism, n = 9; malignancy, n = 7; insufficient follow-up data, n = 1), yielding 74 patients. Paired ventilation imaging was available in 46 patients. STDIBH, short-time deep-inspiratory breath-hold; SPECT/CT, single-photon emission computed tomography/computed tomography.

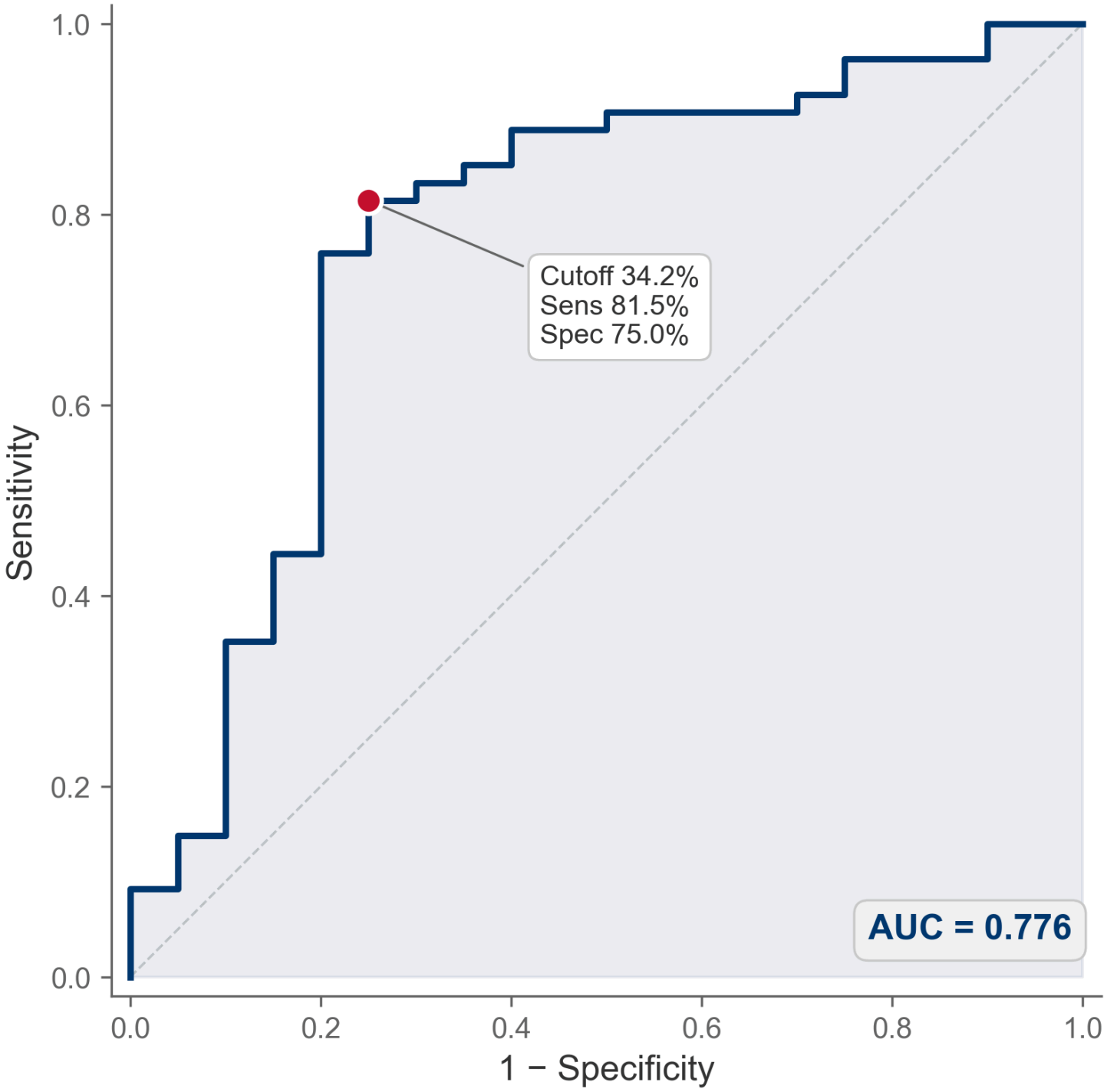
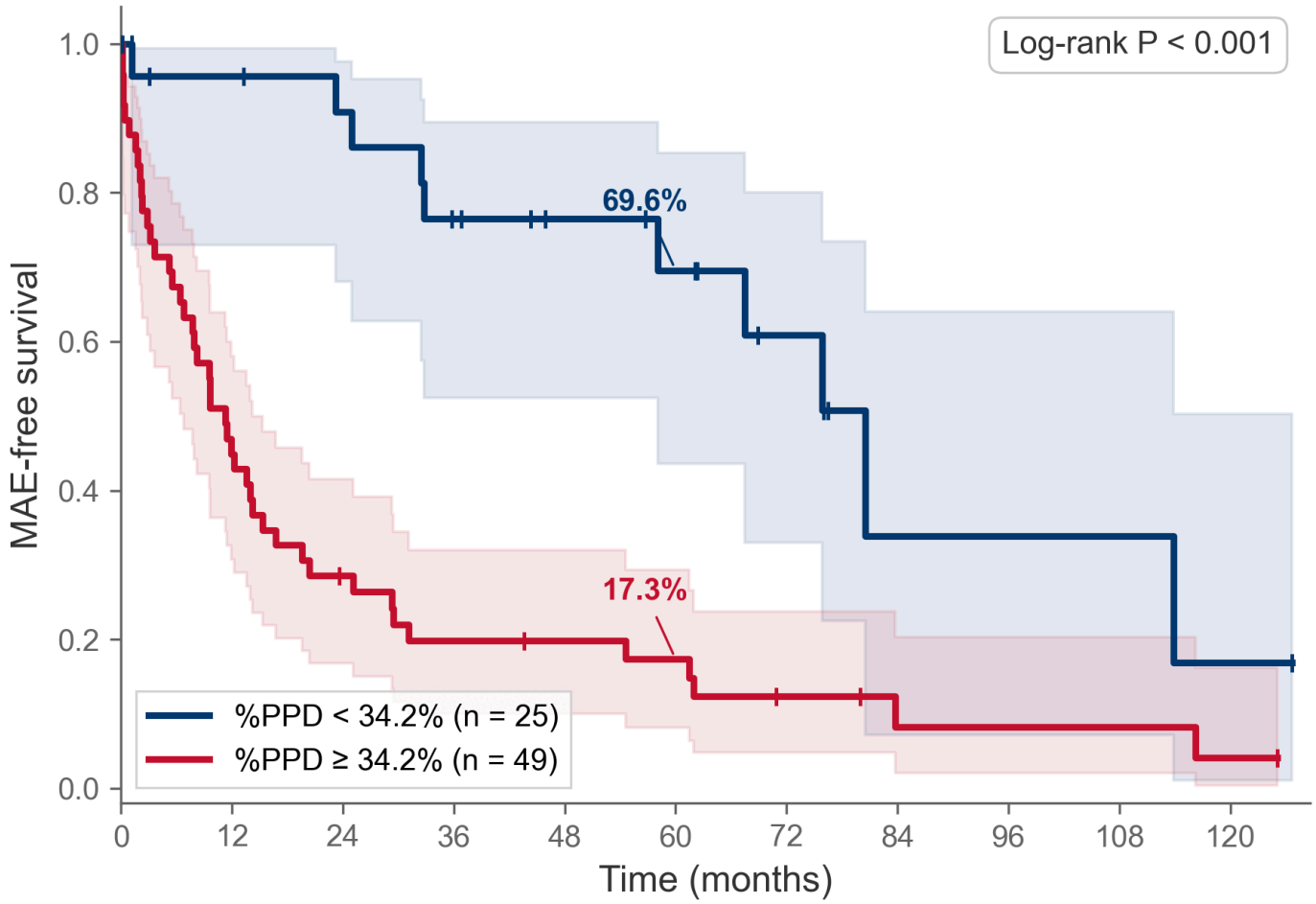



**Figure 2**

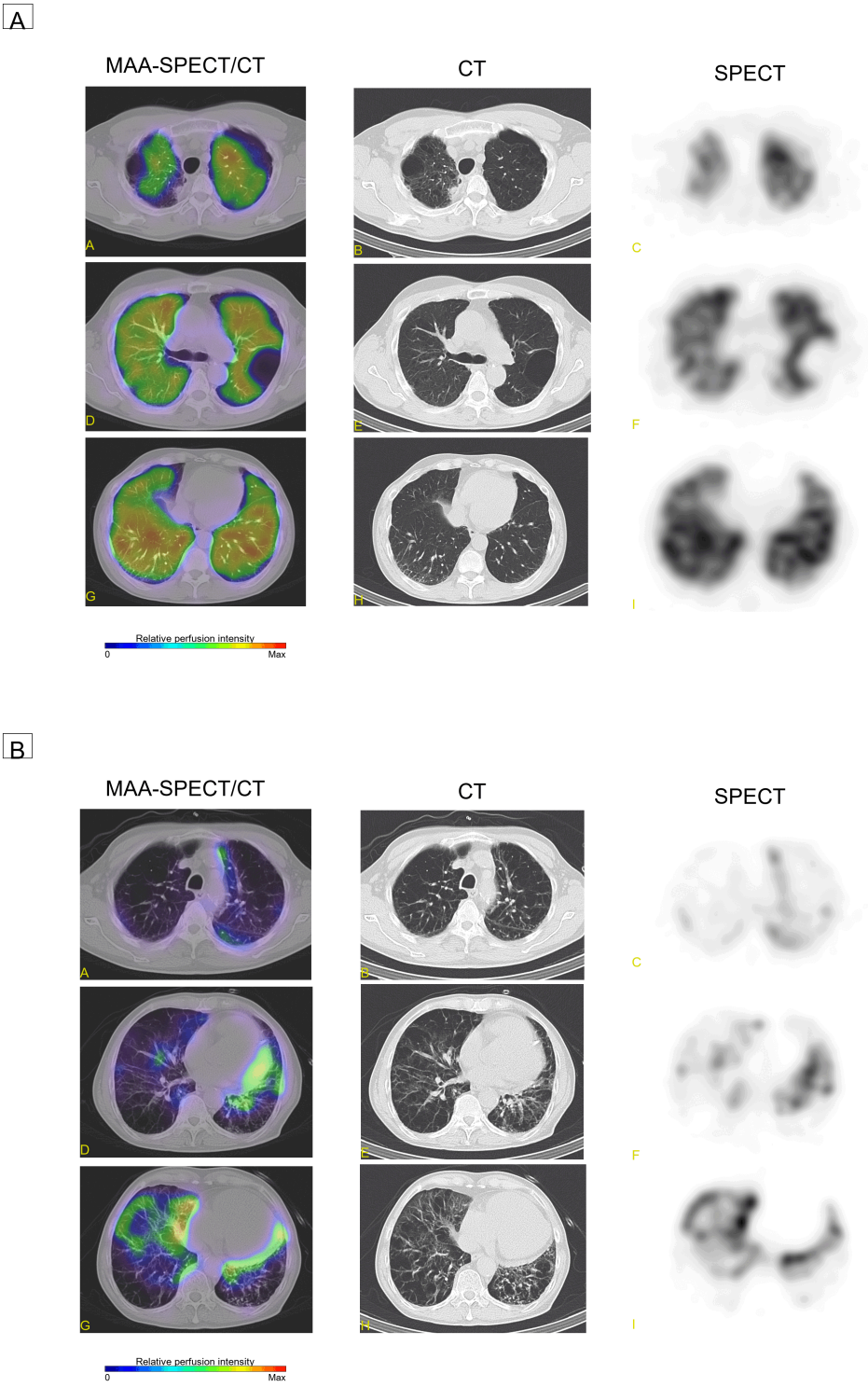
ROC curve for %PPD in predicting MAE (n = 74). AUC = 0.776 (95% CI 0.64–0.90). The Youden-index cutoff was 34.2% (sensitivity 81.5%, 95% CI 69.2–89.6; specificity 75.0%, 95% CI 53.1–88.8). The cutoff was derived in this dataset and requires external validation.




| No. at risk | | | | | | | | | | | |
|---|---|---|---|---|---|---|---|---|---|---|---|
| Low | 25 | 21 | 19 | 15 | 12 | 10 | 6 | 2 | 2 | 2 | 1 |
| High | 49 | 22 | 13 | 9 | 8 | 7 | 4 | 2 | 2 | 2 | 1 |

**Figure 3**

Kaplan-Meier curves for MAE-free survival by %PPD group over the full follow-up. The high %PPD group (≥ 34.2%, n = 49) had worse survival than the low %PPD group (< 34.2%, n = 25; median 11.3 vs 80.6 months, log-rank *P* < 0.001). Number-at-risk values are shown at yearly intervals.




## Figure 4

Representative STDIBH pulmonary perfusion SPECT/CT images illustrating perfusion–structure dissociation. Fusion MAA-SPECT/CT (A, D, G); CT (B, E, H); and SPECT (C, F, I) are shown at three levels with a relative rainbow intensity scale. **Case 1 (low STDIBH-%PPD group):** A 58-year-old man had %LAA 16.0%, %PPD 20.7%, mismatch 4.7%, and 76-month MAE-free follow-up. **Case 2 (high STDIBH-%PPD group):** A 65-year-old man had %LAA 39.0%, %PPD 81.0%, mismatch 42.0%, AECOPD hospitalization at 9.6 months, and death at 43.6 months.

## Supplementary Files

This is a list of supplementary files associated with this preprint. Click to download.

- CRediTstatement.docx
- STROBEChecklist.docx